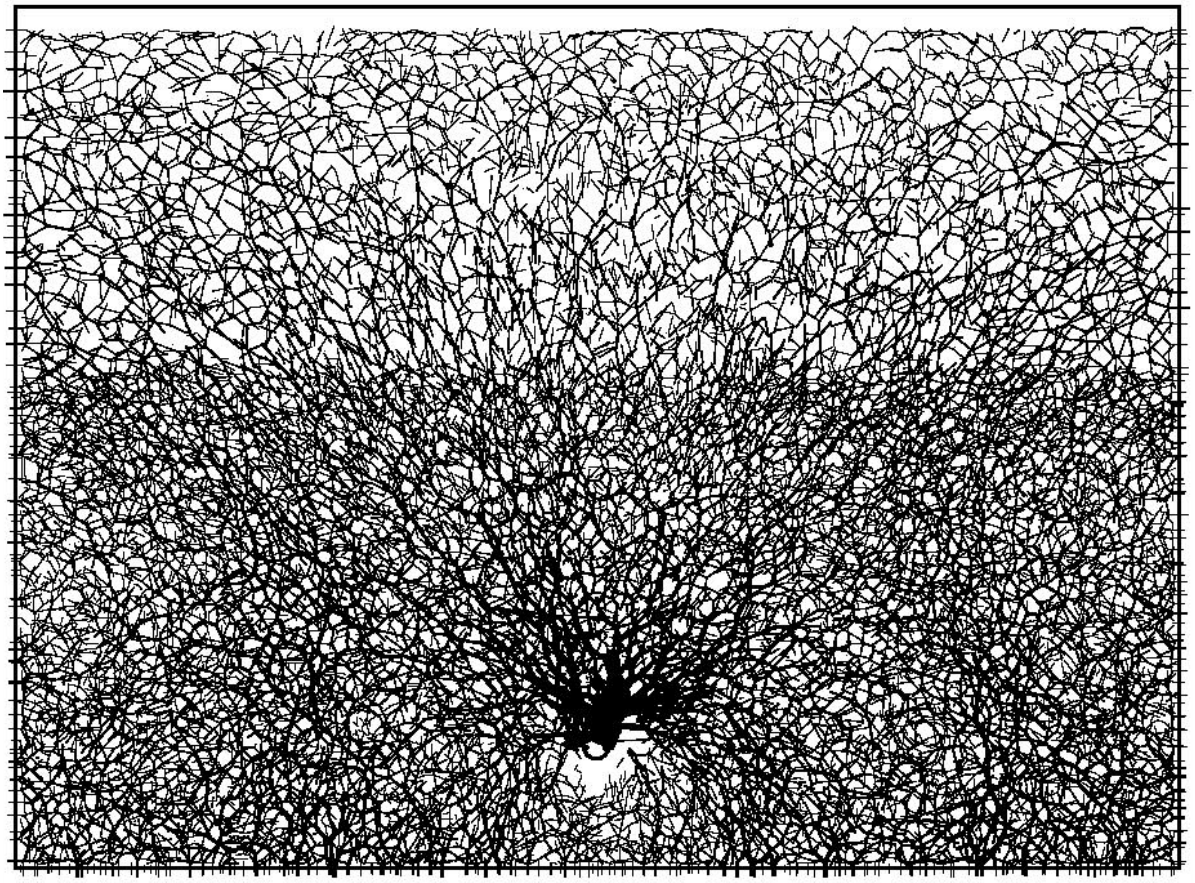

Figure F-13 H_c/D = 30, Dense sand, tan ϕ_μ = 3.0

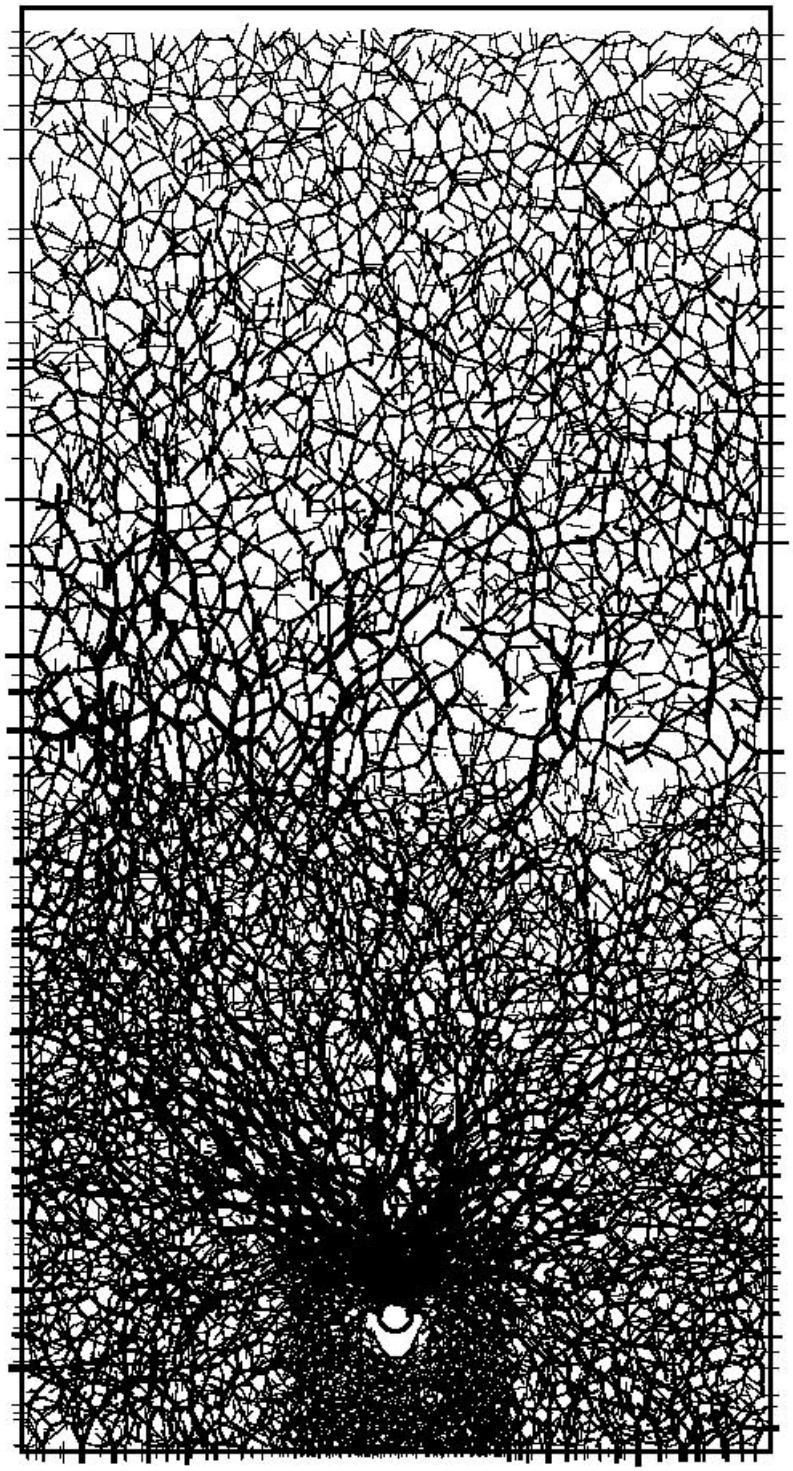

Figure F-14 H_c/D = 40, Medium sand, tan ϕ_μ = 3.0

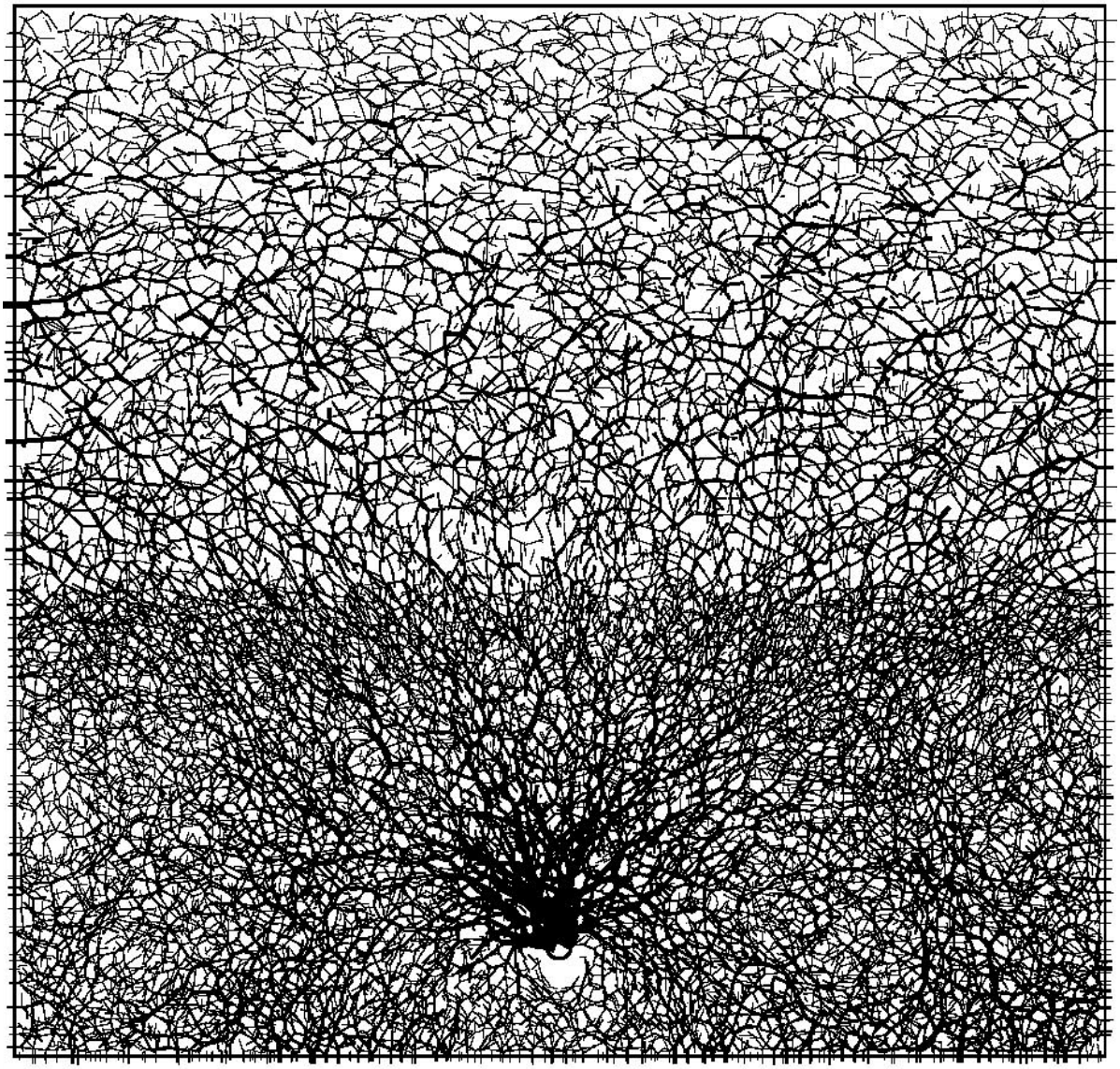

Figure F-15 H_c/D = 40, Dense sand, tan ϕ_μ = 3.0

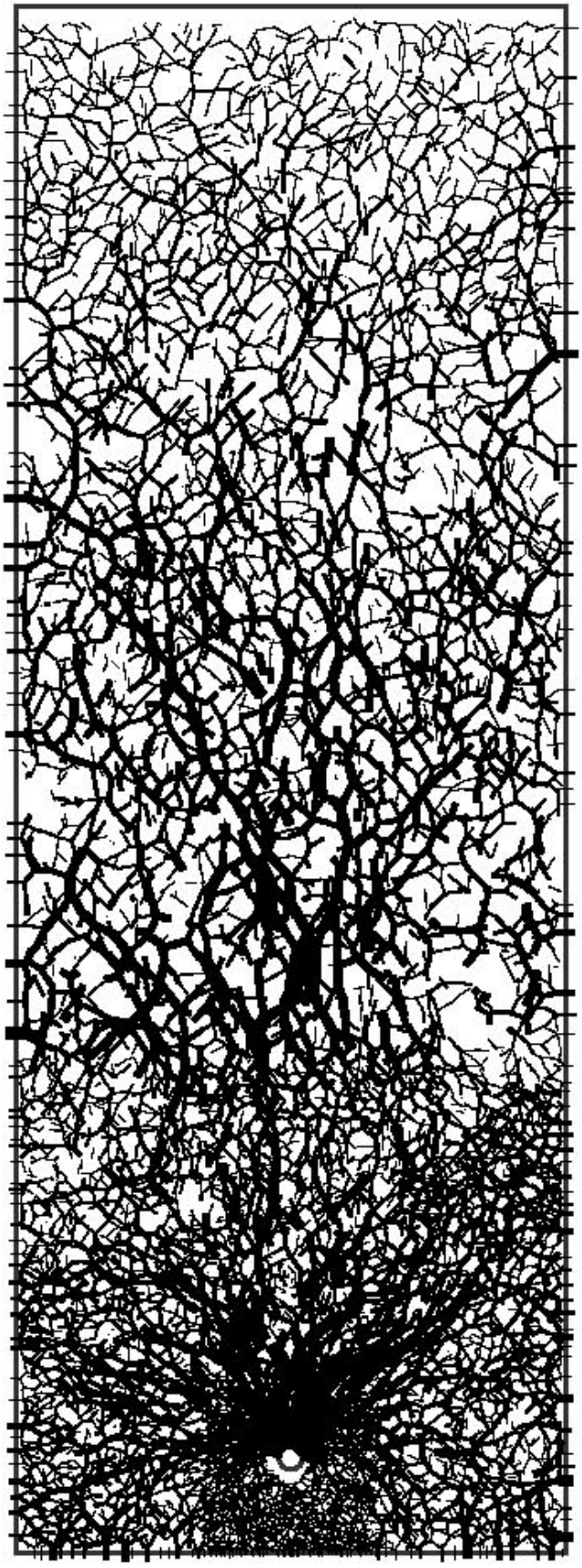

Figure F-16 H_c/D = 60, Medium sand, tan ϕ_μ = 3.0

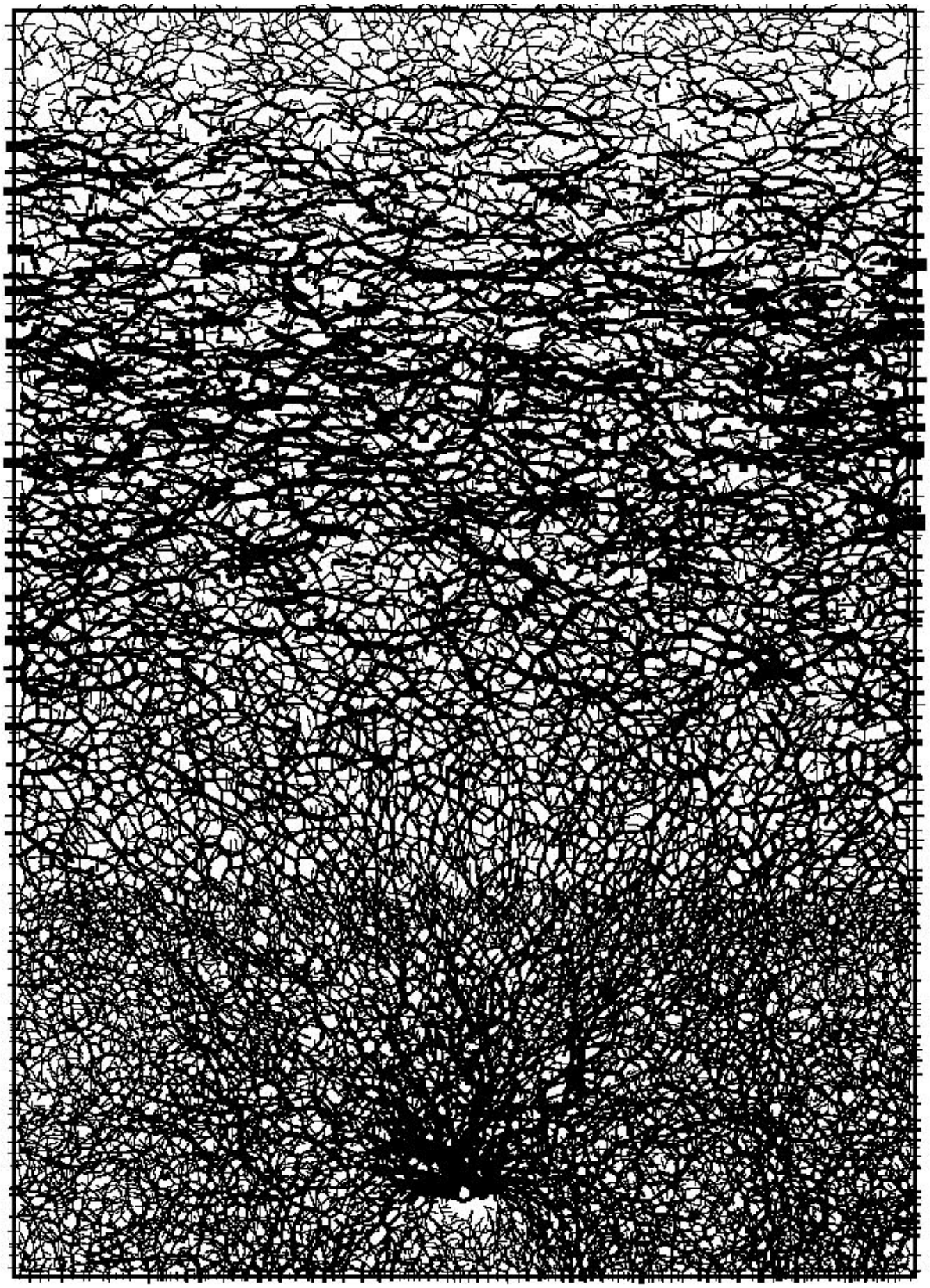

Figure F-17 H_c/D = 60, Dense sand, tan ϕ_μ = 3.0

Appendix G

Parametric Study of DEM Simulation of Triaxial Test

Appendix G

Parametric study of DEM simulation of triaxial test

G.1 General

Parametric study was carried out to examine the effects of the key parameters on the DEM simulation of triaxial tests. The results of this study are presented in this appendix.

G.2 DEM simulation of triaxial test

The triaxial test Test D-2 (CIDC) by Turner & Kulhawy (1987) was used as a controlled test for this study. The nonuniform-sized particles contained within six rigid boundary walls were used as a simulated soil specimen. The particle size of sands follows normal distribution with an average diameter of 5 cm and standard deviation of 1 cm. The specimen size is 1 m by 1 m section and 2 m high. The specimen size was chosen to be relatively large compared with the particle size and accommodated 2402 particles. Fig. G-1 shows the specimen before compression shearing stage. Triaxial test are simulated by moving the top and bottom walls at a specified strain-rate while using servo-controlled to maintain specified stress of the side walls. The parameters of interested are (i) normal contact stiffness, (ii) tangential contact stiffness, and (iii) inter-particle friction angle. The detail of each test is shown in Table G-1. The triaxial test results of Test A (control test) are shown in Fig. G-2.

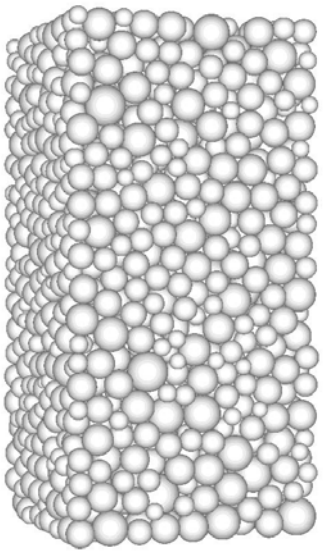

Figure G-1 Specimen before shearing (Test A)

Table G-1 Test details for parametric study

Test No.	p_o' (kPa)	e_o (after consoln)	$k_{N,sand}$ (N/m)	$k_{T,sand}$ (N/m)	tan ϕ_μ	$k_{N,wall}$ (N/m)
Test A*	69	0.490	1.0×10^6	1.0×10^6	1.0	1.0×10^5
Test B	69	0.541	1.0×10^7	1.0×10^6	1.0	1.0×10^5
Test C	69	0.513	1.0×10^6	1.0×10^7	1.0	1.0×10^5
Test D	69	0.497	1.0×10^6	1.0×10^6	5.0	1.0×10^5

Note: tan ϕ_{wall} = 0.0
$k_{T,wall}$ = 0.0
* control test

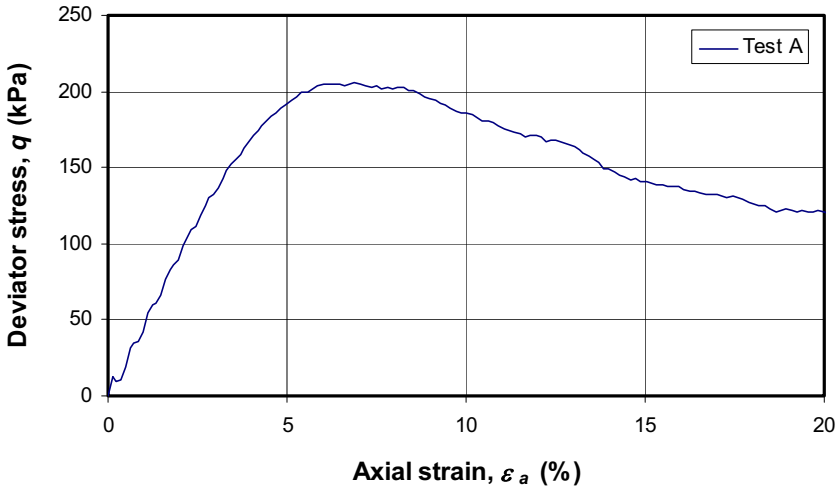

(a) Stress-strain relationship

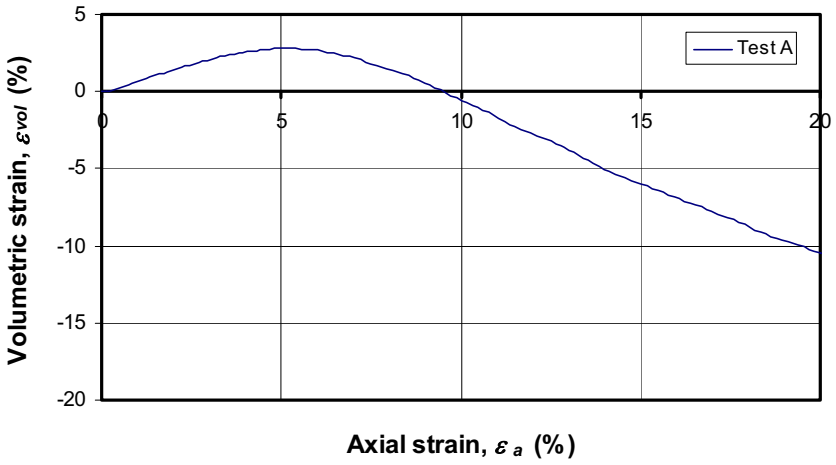

(b) Volumetric strain – axial strain relationship

Figure G-2 Control test (Test A)

G-3 Effects of normal contact stiffness

The effects of normal contact stiffness on triaxial test results are shown in Fig. G-3 by comparing the results of Test A ($k_{N,sand}$ = 1.0 × 10^6 N/m) with Test B ($k_{N,sand}$ = 1.0 × 10^7 N/m). The results show that the normal contact stiffness affects the stiffness from triaxial test without affecting the strength. Fig. G-3(a) shows that, as the normal contact stiffness increases, the stiffness from triaxial test also increases, as can be seen that the slope of the stress-strain curve before failure becomes steeper, with relatively unchanged in peak strength. The strength from Test B is slightly smaller than that from Test A because Test B has slightly larger void ratio (see Table G-1). Fig. G-3(b) shows that, as the normal contact stiffness increases, the specimen becomes more dilative.

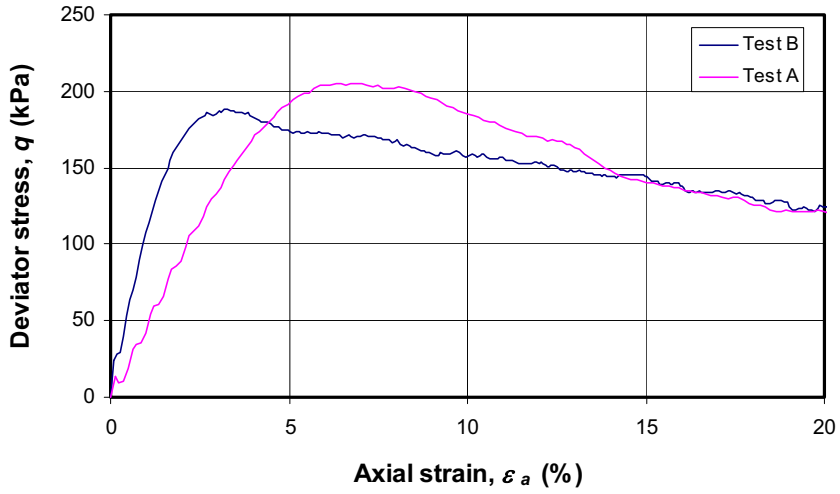

(a) Stress-strain relationship

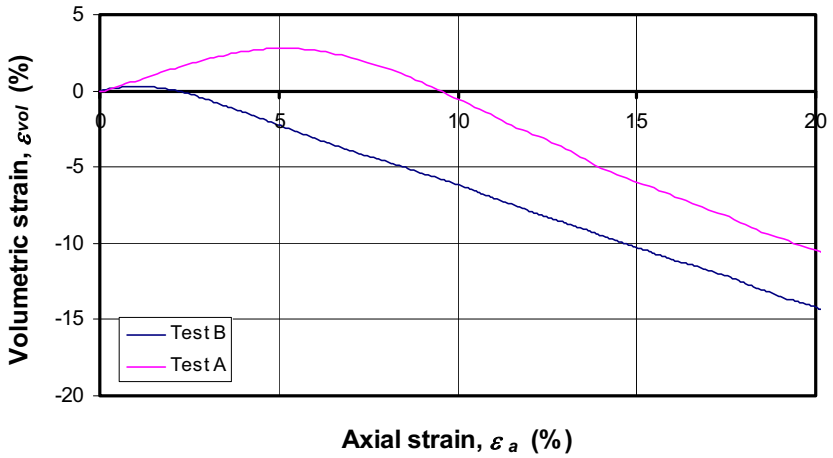

(b) Volumetric strain – axial strain relationship

Figure G-3 Effects of normal contact stiffness

G-4 Effects of tangential contact stiffness

The effects of tangential contact stiffness on triaxial test results are shown in Fig. G-4 by comparing the results of Test A ($k_{T,sand}$ = 1.0 × 10^6 N/m) with Test C ($k_{T,sand}$ = 1.0 × 10^7 N/m). The results show that the change in tangential contact stiffness (within the range studied) has negligible effects on the triaxial test results for both strength and volume change behavior.

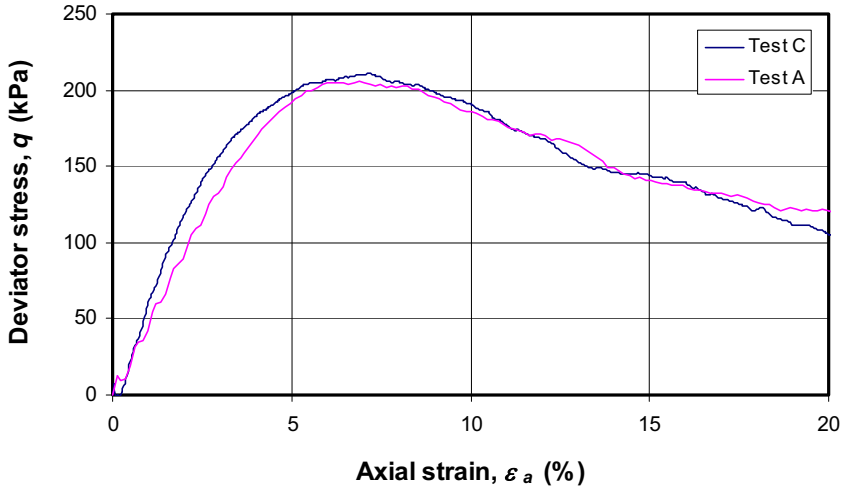

(a) Stress-strain relationship

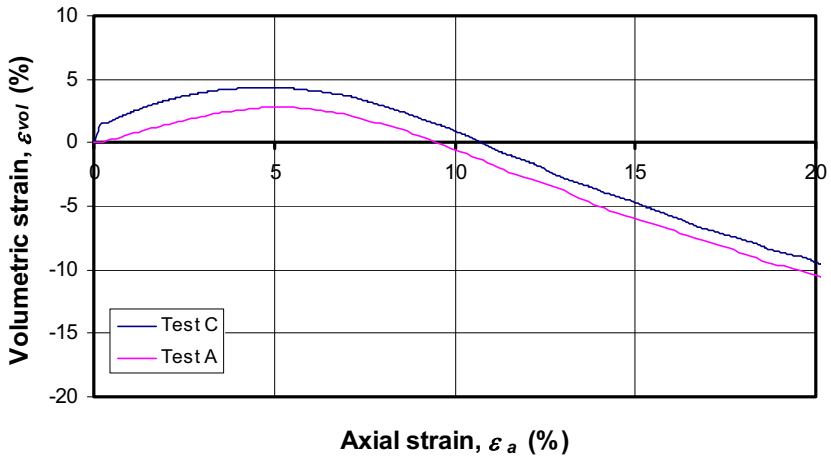

(b) Volumetric strain – axial strain relationship

Figure G-4 Effects of tangential contact stiffness

G-5 Effects of inter-particle friction angle

The effects of inter-particle friction angle on triaxial test results are shown in Fig. G-5 by comparing the results of Test A (tan $\phi_\mu = 1.0$ or $\phi_\mu = 45°$) with Test D (tan $\phi_\mu = 5.0$ or $\phi_\mu = 79°$). Fig. G-5(a) shows that the inter-particle friction angle affects the strength from triaxial test without affecting the stiffness. As the inter-particle friction angle increases, the peak strength becomes larger with relatively unchanged in triaxial stiffness, as can be seen from the unchanged slope of the stress-strain curve before failure. Fig. G-5(b) shows that the inter-particle friction angle does not show obvious effects on the volume change behavior. As the inter-particle friction angle increases, the dilation behavior is still unchanged at small strain, becomes less dilative (more compressive) at intermediate strain, and becomes more dilative at large strain.

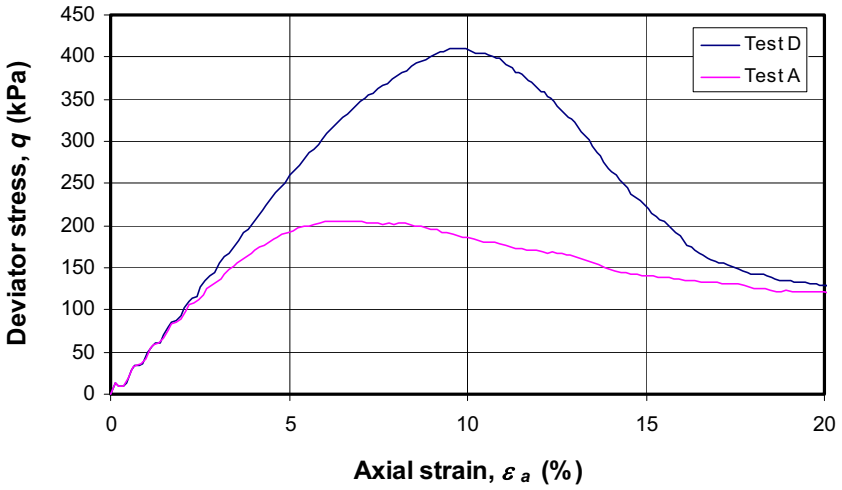

(a) Stress-strain relationship

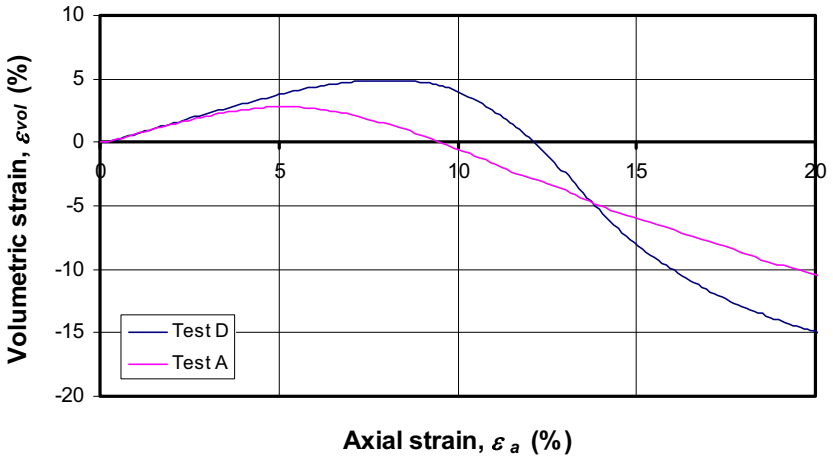

(b) Volumetric strain – axial strain relationship

Figure G-5 Effects of inter-particle friction angle

G-6 Summary

The results of the parametric study can be summarized as shown in Table G-2.

Table G-2 Results of parametric study of triaxial test

Microscopic parameters	Effects on macroscopic parameters when the values of microscopic parameter increases		
	Triaxial stiffness	Triaxial strength	Dilation
Normal contact stiffness	↑	—	↑
Tangential contact stiffness	—	—	—
Inter-particle friction angle	—	↑	inconclusive

where — = negligible change
↑ = increase
↓ = decrease

Appendix H

Parametric Study of DEM Simulation of Lateral Pipe Loading

Appendix H

Parametric study of DEM simulation of lateral pipe loading

H.1 General

Parametric studies were carried out to examine the effects of key parameters on the DEM analysis results of lateral pipe loading. The case of medium sand with H/D = 11.5 was selected for a parametric study. The parameters investigated include normal contact stiffness of particle, tangential contact stiffness of particle, inter-particle friction angle, normal contact stiffness of pipe, tangential contact stiffness of pipe, pipe surface friction angle, pipe pulling velocity, and extent of fine particles. The input parameters for the parametric study are shown in Table H-1. The DEM analysis result of the control test is shown in Figure H-1.

Table H-1 Input parameters for parametric study of lateral pipe loading

Parameters	Test A*	Test B	Test C	Test D	Test E	Test F	Test G	Test H	Test I
Particle normal contact stiffness, $k_{N,sand}$ (N/m)	5.0×10^5	2.5×10^6	5.0×10^5	5.0×10^5	5.0×10^5	5.0×10^5	5.0×10^5	5.0×10^5	5.0×10^5
Particle tangential contact stiffness, $k_{T,sand}$ (N/m)	5.0×10^5	5.0×10^5	2.5×10^6	5.0×10^5	5.0×10^5	5.0×10^5	5.0×10^5	5.0×10^5	5.0×10^5
Inter-particle friction angle, tan ϕ_μ	1.0	1.0	1.0	3.0	1.0	1.0	1.0	1.0	1.0
Pipe normal contact stiffness, $k_{N,pipe}$ (N/m)	5.0×10^5	5.0×10^5	5.0×10^5	5.0×10^5	2.5×10^6	5.0×10^5	5.0×10^5	5.0×10^5	5.0×10^5
Pipe tangential contact stiffness, $k_{T,pipe}$ (N/m)	5.0×10^5	5.0×10^5	5.0×10^5	5.0×10^5	5.0×10^5	2.5×10^6	5.0×10^5	5.0×10^5	5.0×10^5
Pipe surface friction, tan ϕ_{pipe}	0.41	0.41	0.41	0.41	0.41	0.41	1.0	0.41	0.41
Pipe pulling velocity, V (m/s)	0.3	0.3	0.3	0.3	0.3	0.3	0.3	0.15	0.3
Extent of fine particles (as shown in Fig. 4-3)	✓	✓	✓	✓	✓	✓	✓	✓	✗

* control test

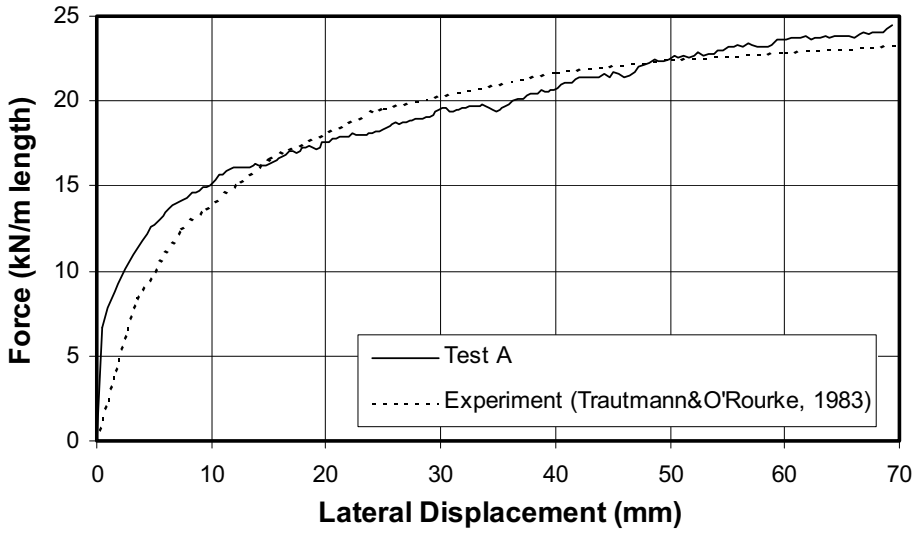

(a) Force – displacement relationship

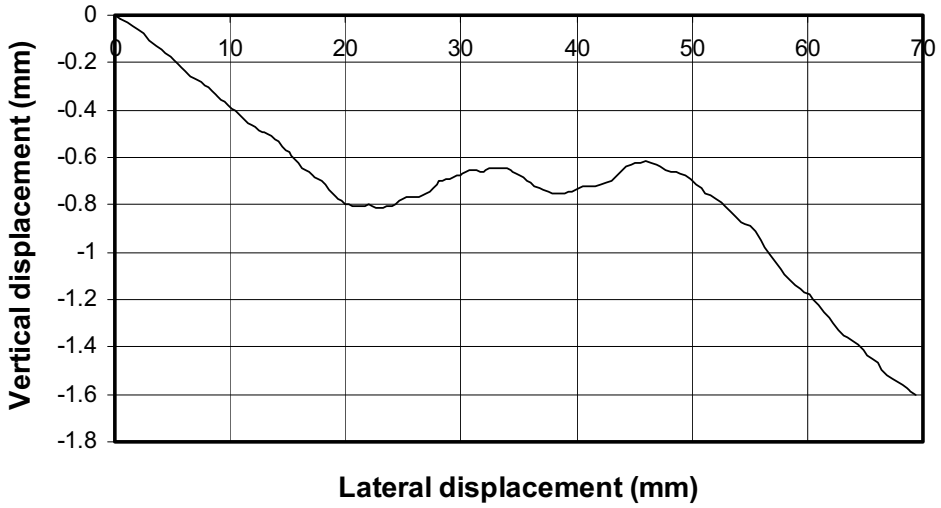

(b) Vertical –lateral displacement relationship

Figure H-1 Control test (Test A)

H-2 Effects of particle normal contact stiffness

The effects of particle normal contact stiffness on lateral pipe loading results are shown in Fig. H-2 by comparing the results of Test A ($k_{N,sand}$ = 5.0 × 10^5 N/m) with Test B ($k_{N,sand}$ = 2.5 × 10^6 N/m (increased by 5 times)). The results show that the peak force becomes larger as the particle normal contact stiffness increases. This is contrary to the effects of particle

contact stiffness on the triaxial test results which show that contact stiffness affects only stiffness (modulus) but not strength (see Appendix G). This may be due to the more complex mode of shearing in pipe loading problem.

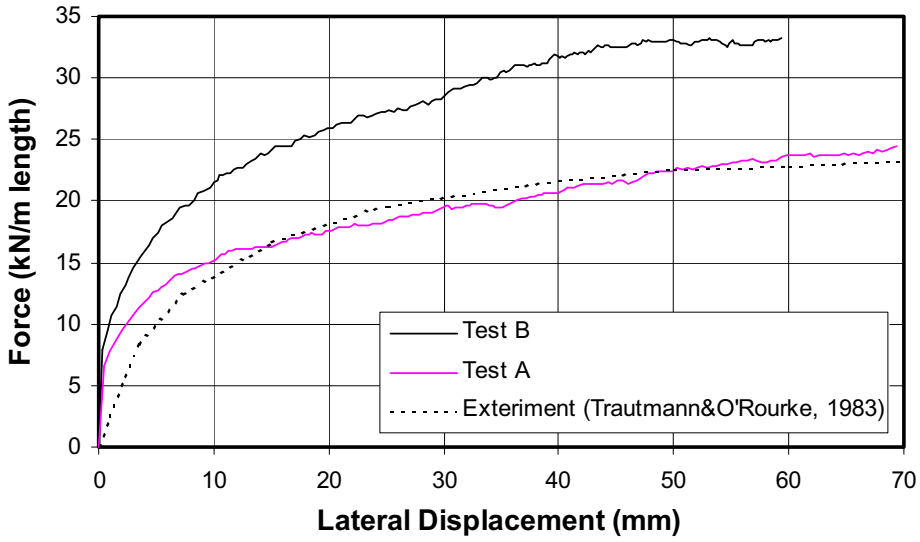

(a) Force – displacement relationship

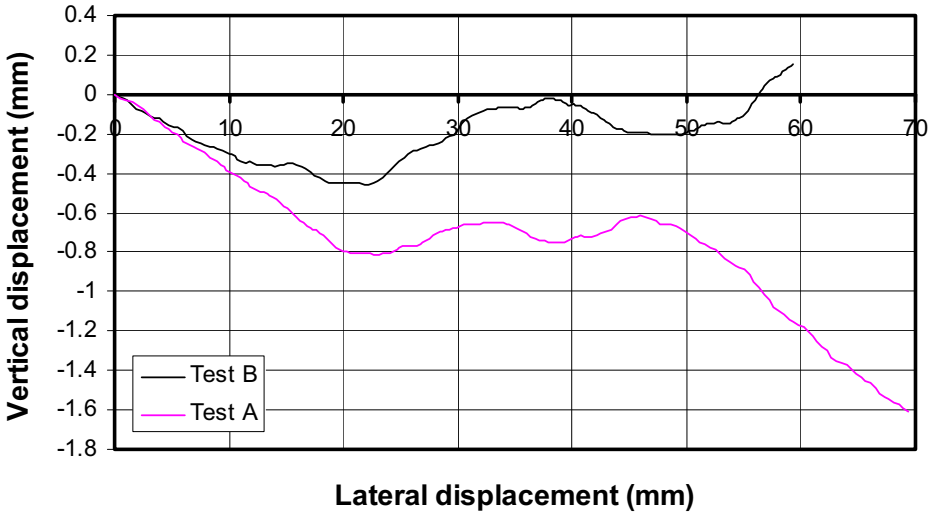

(b) Vertical –lateral displacement relationship

Figure H-2 Effects of particle normal contact stiffness

H-3 Effects of particle tangential contact stiffness

The effects of particle tangential contact stiffness on lateral pipe loading results are shown in Fig. H-3 by comparing the results of Test A ($k_{T,sand}$ = 5.0 × 10^5 N/m) with Test C ($k_{T,sand}$ = 2.5 × 10^6 N/m (increased by 5 times)). The results show that the change in particle tangential contact stiffness (within the range studied) has minimal effects on the lateral pipe loading results.

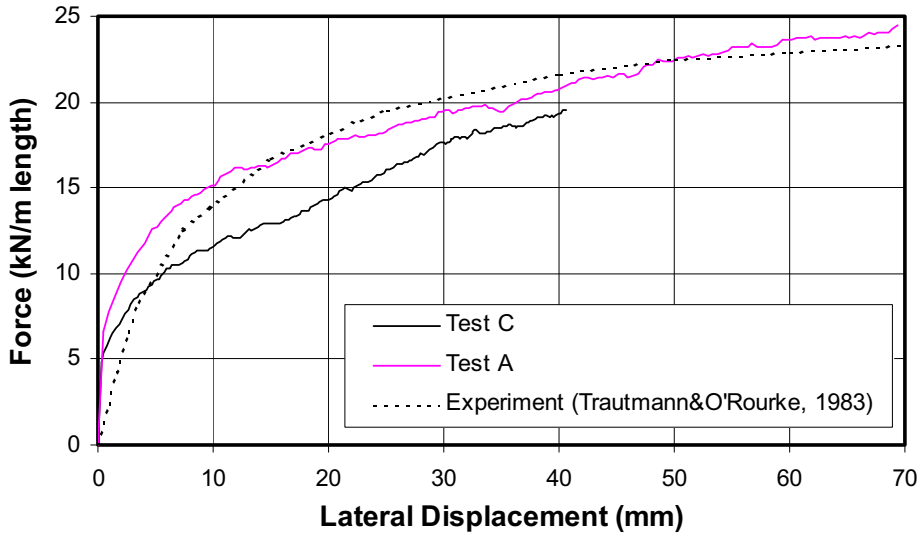

(a) Force – displacement relationship

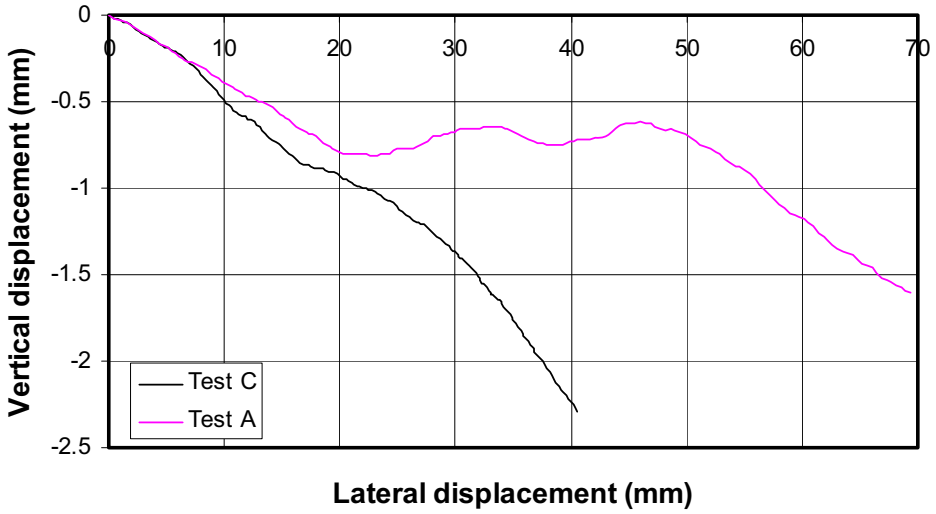

(b) Vertical –lateral displacement relationship

Figure H-3 Effects of particle tangential contact stiffness

H-4 Effects of inter-particle friction angle

The effects of inter-particle friction angle on lateral pipe loading results are shown in Fig. H-4 by comparing the results of Test A (tan ϕ_μ = 1.0 or ϕ_μ = 45°) with Test D (tan ϕ_μ = 3.0 or ϕ_μ = 72°). The results show that the peak force becomes larger as the inter-particle friction angle increases. This is consistent with the effects of inter-particle friction angle on triaxial test results which show that an increase in the inter-particle friction angle yields an increase in strength (see Appendix G).

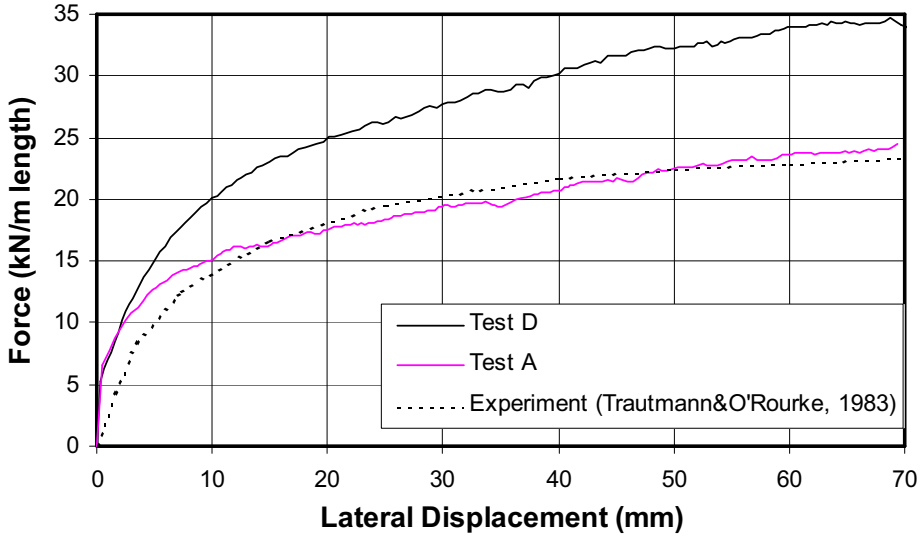

(a) Force – displacement relationship

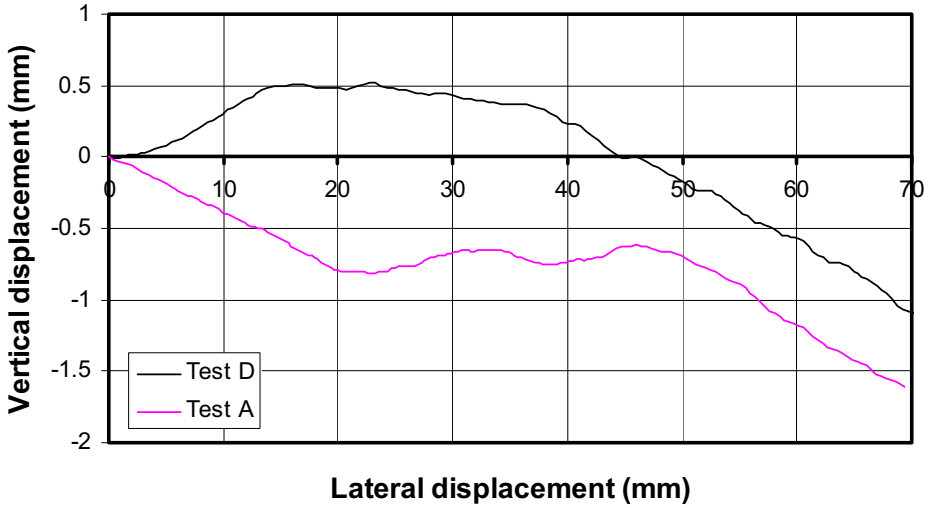

(b) Vertical –lateral displacement relationship

Figure H-4 Effects of inter-particle friction angle

H-5 Effects of pipe normal contact stiffness

The effects of pipe normal contact stiffness on lateral pipe loading results are shown in Fig. H-5 by comparing the results of Test A ($k_{N,pipe}$ = 5.0 × 10^5 N/m) with Test E ($k_{N,pipe}$ = 2.5 × 10^6 N/m (increased by 5 times)). The results show that the change in pipe normal contact stiffness (within the range studied) has negligible effects on the lateral pipe loading results. In the present DEM analysis, the pipe normal contact stiffness is equal to the particle normal contact stiffness.

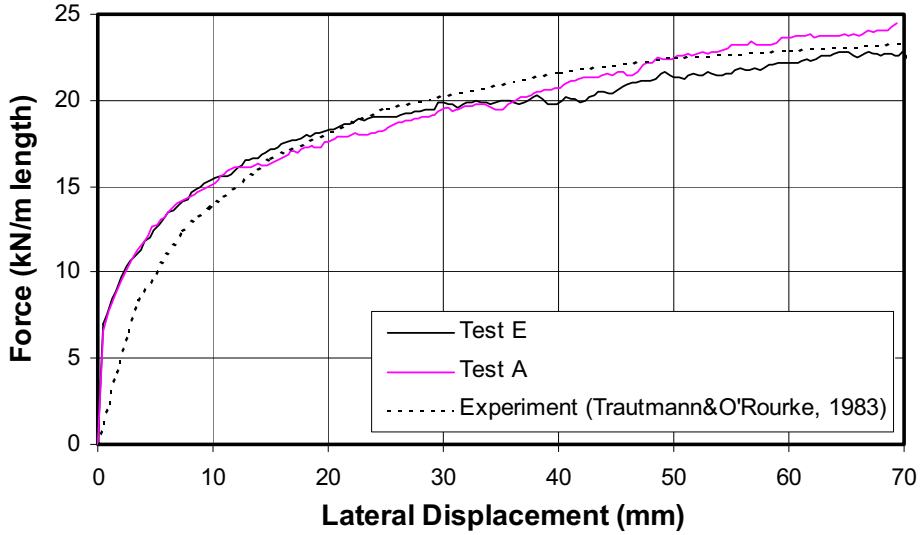

(a) Force – displacement relationship

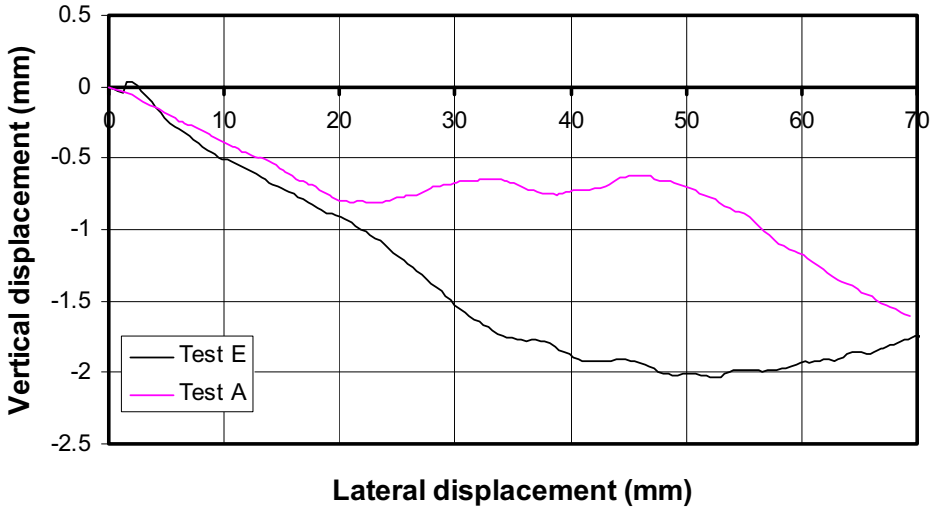

(b) Vertical –lateral displacement relationship

Figure H-5 Effects of pipe normal contact stiffness

H-6 Effects of pipe tangential contact stiffness

The effects of pipe tangential contact stiffness on lateral pipe loading results are shown in Fig. H-6 by comparing the results of Test A ($k_{T,pipe}$ = 5.0 × 10^5 N/m) with Test F ($k_{T,pipe}$ = 2.5 × 10^6 N/m (increased by 5 times)). The results show that the change in pipe tangential contact stiffness (within the range studied) has negligible effects on the lateral pipe loading results. In the present DEM analysis, the pipe tangential contact stiffness is equal to the pipe normal contact stiffness.

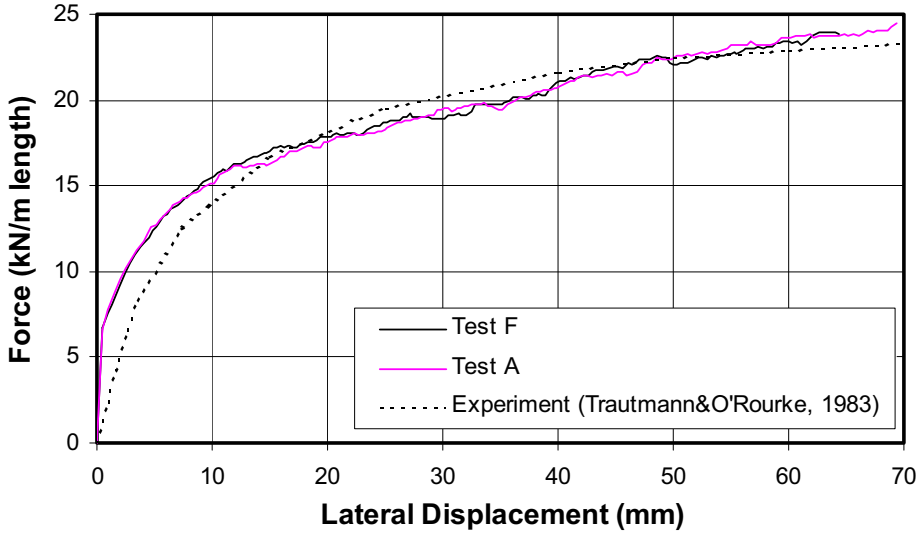

(a) Force – displacement relationship

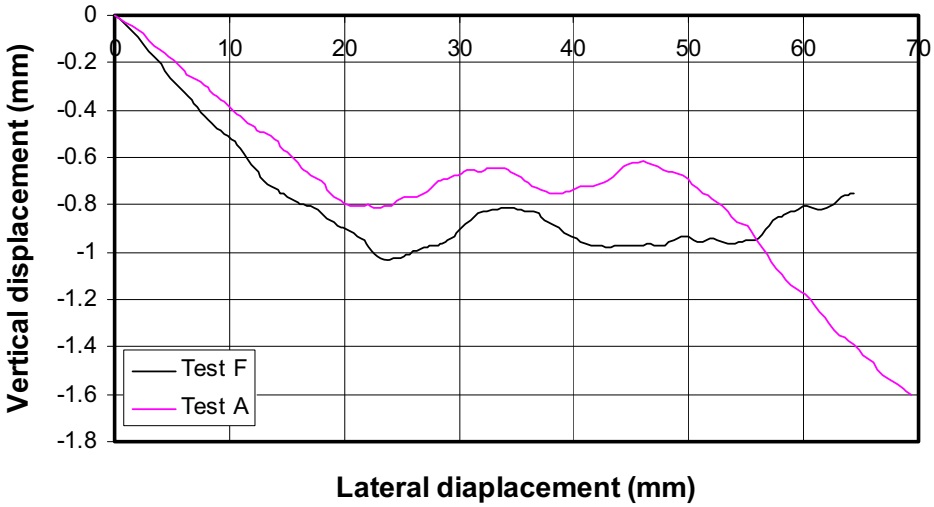

(b) Vertical –lateral displacement relationship

Figure H-6 Effects of pipe tangential contact stiffness

H-7 Effects of pipe surface friction

The effects of pipe surface friction on lateral pipe loading results are shown in Fig. H-7 by comparing the results of Test A (tan ϕ_{pipe} = 0.41 or $\phi_{pipe} = \phi_{\mu}/2$) with Test G (tan ϕ_{pipe} = 1.0 or $\phi_{pipe} = \phi_{\mu}$). The results show that the change in pipe surface friction (between $\phi_{pipe} = \phi_{\mu}/2$ and $\phi_{pipe} = \phi_{\mu}$) has negligible effects on the lateral pipe loading results.

The pipe surface friction angle ϕ_{pipe} generally ranges from about 20° to a value equal to the friction angle of the soil. The larger values would be characteristic of rough uncoated pipes with rusting or corroded surface and the lower values would correspond to pipes with smooth coatings. The condition of the surface of the pipe in the experiments by Trautmann & O'Rourke (1983) was described as rough, scaly surfaces with minor rust patches. Therefore, the ϕ_{pipe} was assumed to be $\phi_{\mu}/2$ in the present DEM analysis. The real ϕ_{pipe} can probably lie between $\phi_{\mu}/2$ and ϕ_{μ} which gives negligible difference. Rowe & Davis (1982) also suggested that the effects of pipe surface friction is expected to decrease as the depth of the pipe increases. According to their computations, pipe surface roughness has the greatest influence on shallow vertical anchors resisting horizontal forces. The effects were found to be minimal for deep anchors and for anchors resisting uplift forces.

In the present DEM analysis, the sidewall and base of the test tank were assumed to be perfectly smooth. Although Trautmann & O'Rourke (1983) reported that the smooth Formica, which has ϕ_{μ} = 0.6 ϕ_{max}, was used as the sidewall and base, the assumption of smooth sidewall and base is still considered justifiable because the far boundary in the experiment configuration should exclude the boundary effects (except for some cases of dense sand with deep embedment depth). Moreover, since the test tank was made to be relatively wide, the assumption of plane strain condition in the DEM analysis is also justifiable.

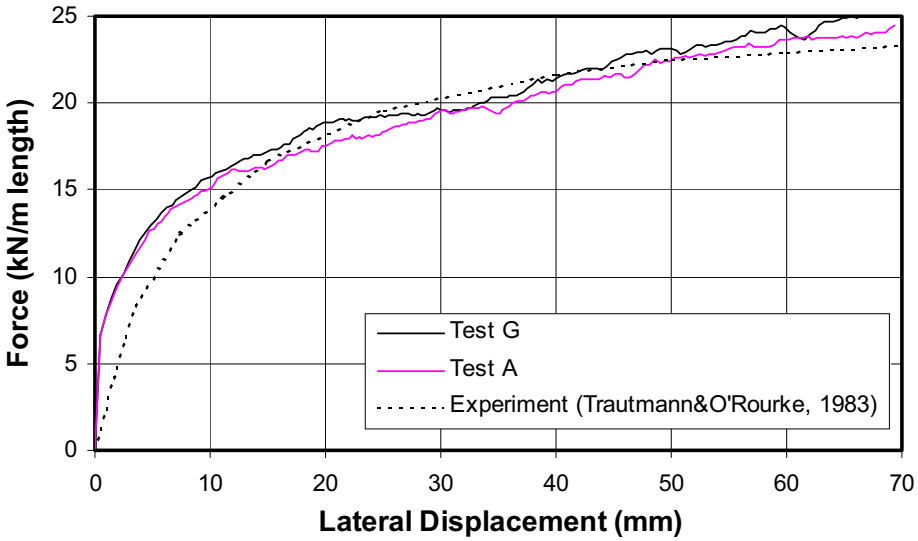

(a) Force – displacement relationship

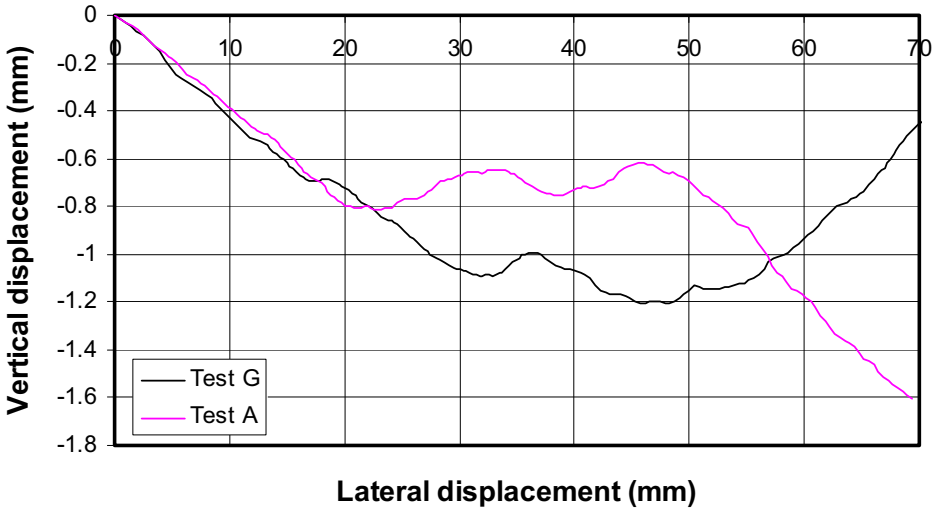

(b) Vertical –lateral displacement relationship

Figure H-7 Effects of pipe surface friction

H-8 Effects of pipe pulling velocity

The effects of pipe pulling velocity on lateral pipe loading results are shown in Fig. H-8 by comparing the results of Test A (V = 0.3 m/s) with Test H (V = 0.15 m/s (reduced by half)). The results show that the decrease in the pipe pulling velocity results in a slight decrease in the peak force (approximately 20% reduction). However, the selection of the pipe pulling velocity must consider the required time to complete the analysis. A slower pipe pulling velocity may give a small decrease in the peak force; however, the selected pipe pulling velocity of 0.3 m/s is consider justifiable considering the required analysis time. Moreover, by default, PFC^{3D} operates in "static" mode – that is, internal damping is applied that causes the system of particles to reach equilibrium in a minimum number of cycles.

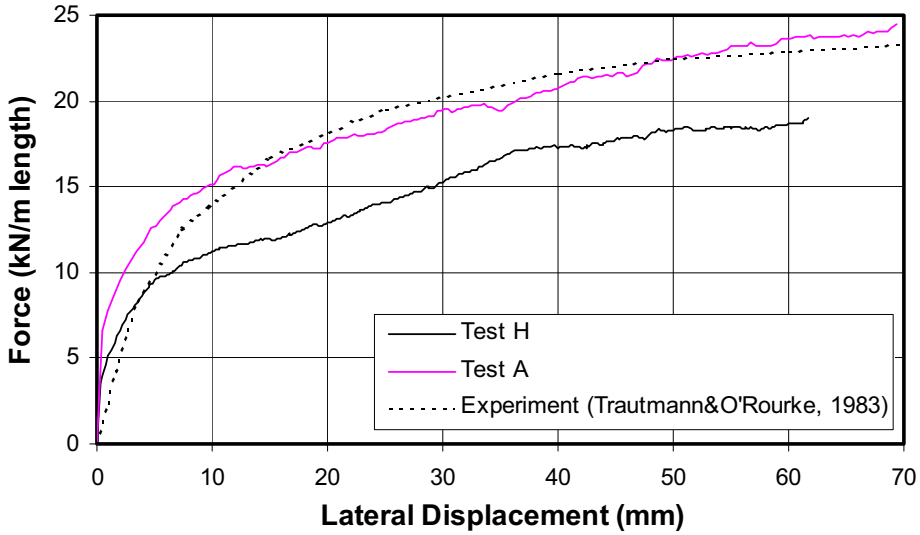

(a) Force – displacement relationship

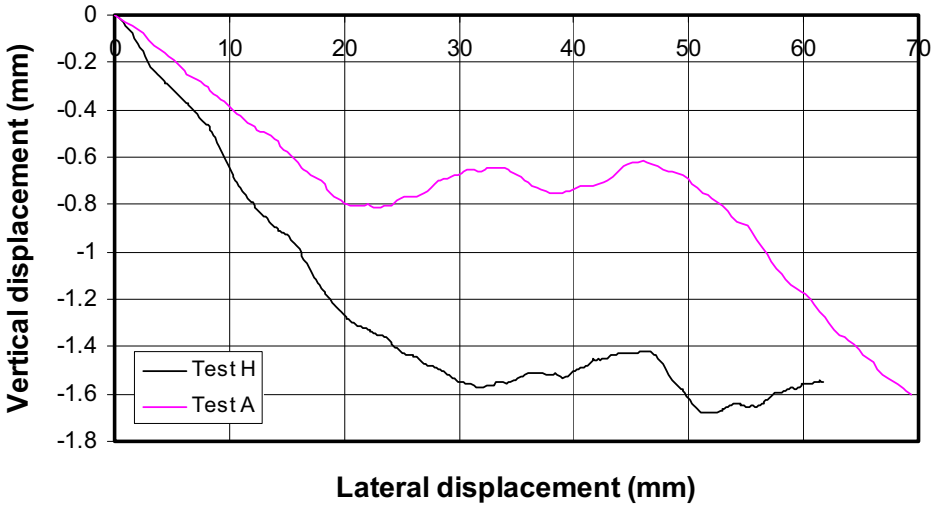

(b) Vertical –lateral displacement relationship

Figure H-8 Effects of pipe pulling velocity

H-9 Effects of extent of fine particle

The effects of extent of fine particle on lateral pipe loading results are shown in Fig. H-9 by comparing the results of Test A (with fine particles (Region A in Fig. 4-3)) with Test I (without fine particles (without Region A in Fig. 4-3)). The results show that the extent of fine particle has minimal effects on the lateral pipe loading results. In the present DEM analysis, the extent of fine particle is included.

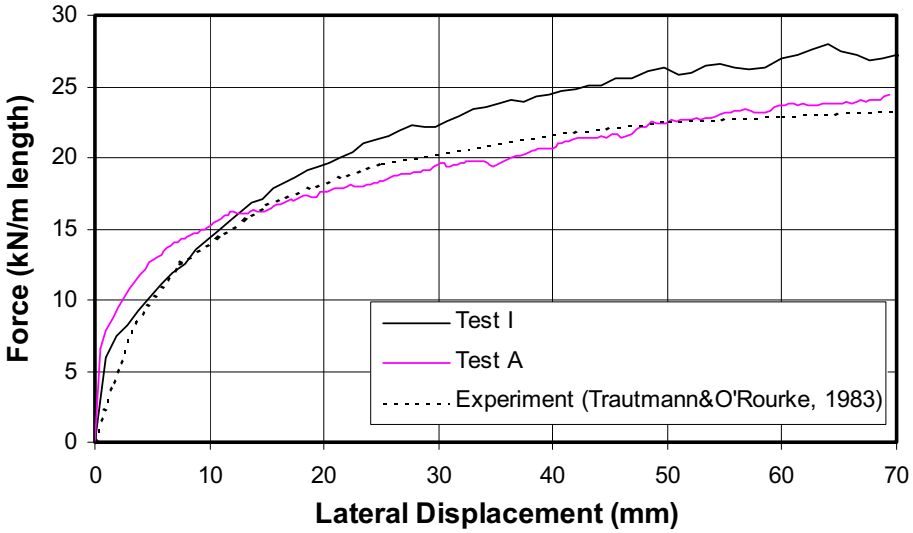

(a) Force – displacement relationship

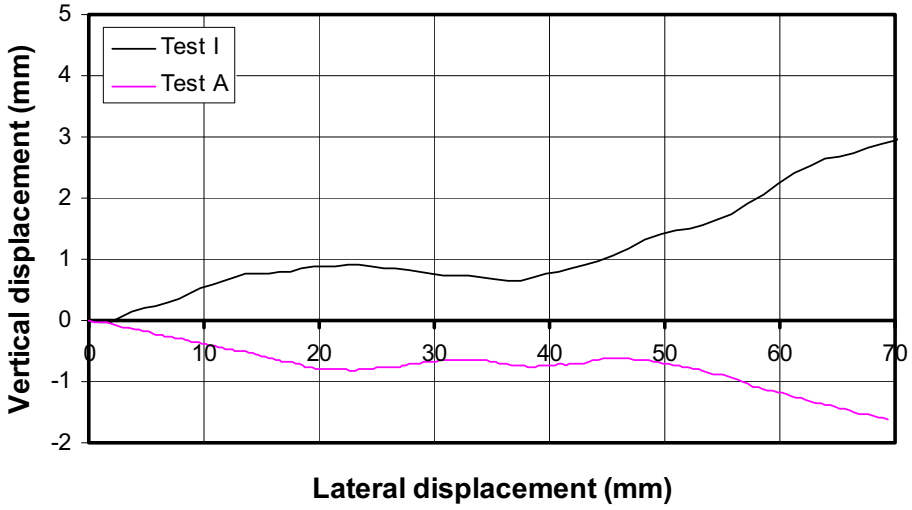

(b) Vertical –lateral displacement relationship

Figure H-9 Effects of extent of fine particle

H-10 Summary

The results of the parametric study can be summarized as shown in Table H-2.

Table H-2 Results of parametric study of lateral pipe loading

Parameters	Effects on peak force when the values of the parameters increase
Particle normal contact stiffness, $k_{N,sand}$ (N/m)	↑
Particle tangential contact stiffness, $k_{T,sand}$ (N/m)	—
Inter-particle friction angle, tan ϕ_μ	↑
Pipe normal contact stiffness, $k_{N,pipe}$ (N/m)	—
Pipe tangential contact stiffness, $k_{T,pipe}$ (N/m)	—
Pipe surface friction, tan ϕ_{pipe}	—
Pipe pulling velocity, V (m/s)	↑ (small)
Extent of fine particles (as shown in Fig. 4-3)	—

where — = negligible change
↑ = increase
↓ = decrease
small = the effects are small

Appendix I

Parametric Study of DEM Simulation of Upward Pipe Loading

Appendix I

Parametric study of DEM simulation of upward pipe loading

I.1 General

Parametric studies were carried out to examine the effects of the key parameters on the DEM analysis results of upward pipe loading. The case of medium sand with H_c/D = 13 was selected for a parametric study. The parameters investigated include normal contact stiffness of particle, tangential contact stiffness of particle, inter-particle friction angle, normal contact stiffness of pipe, tangential contact stiffness of pipe, pipe friction angle, pipe pulling velocity, and extent of fine particle. The input parameters for the parametric study are shown in Table I-1. The DEM analysis result of the control test is shown in Figure I-1.

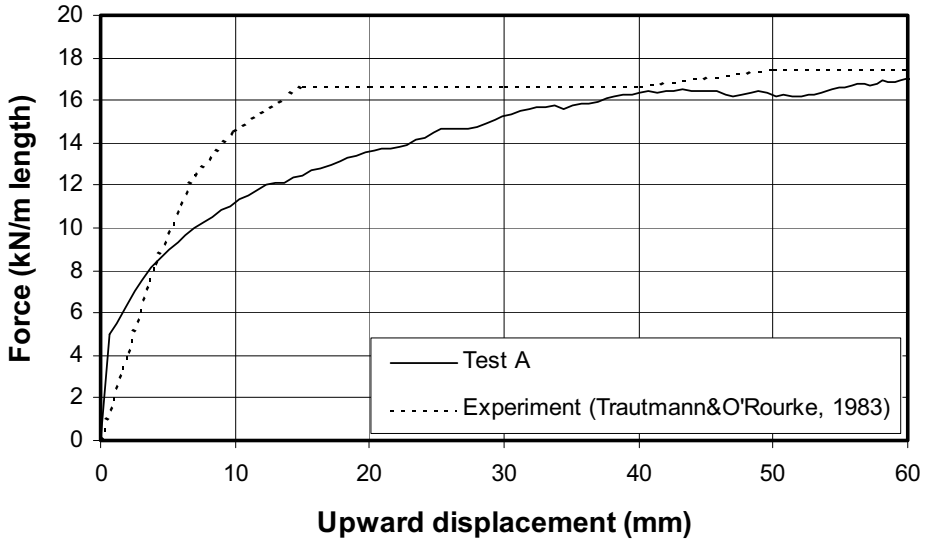

Figure I-1 Control test (Test A)

Table I-1 Input parameters for parametric study of upward pipe loading

Parameters	Test A*	Test B	Test C	Test D	Test E	Test F	Test G	Test H	Test I
Particle normal contact stiffness, $k_{N,sand}$ (N/m)	2.0×10^5	1.0×10^6	2.0×10^5	2.0×10^5	2.0×10^5	2.0×10^5	2.0×10^5	2.0×10^5	2.0×10^5
Particle tangential contact stiffness, $k_{T,sand}$ (N/m)	2.0×10^5	2.0×10^5	1.0×10^6	2.0×10^5	2.0×10^5	2.0×10^5	2.0×10^5	2.0×10^5	2.0×10^5
Inter-particle friction angle, tan ϕ_μ	1.0	1.0	1.0	3.0	1.0	1.0	1.0	1.0	1.0
Pipe normal contact stiffness, $k_{N,pipe}$ (N/m)	2.0×10^5	2.0×10^5	2.0×10^5	2.0×10^5	1.0×10^6	2.0×10^5	2.0×10^5	2.0×10^5	2.0×10^5
Pipe tangential contact stiffness, $k_{T,pipe}$ (N/m)	2.0×10^5	2.0×10^5	2.0×10^5	2.0×10^5	2.0×10^5	1.0×10^6	2.0×10^5	2.0×10^5	2.0×10^5
Pipe surface friction, tan ϕ_{pipe}	0.41	0.41	0.41	0.41	0.41	0.41	1.0	0.41	0.41
Pipe pulling velocity (m/s)	0.3	0.3	0.3	0.3	0.3	0.3	0.3	0.15	0.3
Extent of fine particle (as shown in Fig. 4-3)	✓	✓	✓	✓	✓	✓	✓	✓	✗

* control test